The Wave Kernel Signature:
A Quantum Mechanical Approach to Shape Analysis

Mathieu Aubry, Ulrich Schlickewei and Daniel Cremers
Department of Computer Science, TU München

Abstract

We introduce the Wave Kernel Signature (WKS) for characterizing points on non-rigid three-dimensional shapes. The WKS represents the average probability of measuring a quantum mechanical particle at a specific location. By letting vary the energy of the particle, the WKS encodes and separates information from various different Laplace eigenfrequencies. This clear scale separation makes the WKS well suited for a large variety of applications. Both theoretically and in quantitative experiments we demonstrate that the WKS is substantially more discriminative and therefore allows for better feature matching than the commonly used Heat Kernel Signature (HKS). As an application of the WKS in shape analysis we show results on shape matching.

1. Feature Descriptors for Shape Analysis

The central component in the analysis of three-dimensional shapes is a *feature descriptor* which characterizes each point on the object's surface regarding its relation to the entire shape. The key idea is to associate with each point on a surface in $\mathbb{R}^3$ a feature vector in $\mathbb{R}^n$ or more generally a scalar function on $\mathbb{R}$ which ideally contains all relevant local and global information about this point.

In *shape matching* this descriptor is used for detecting potential correspondences among pairs of points on either shape. In *shape segmentation* the descriptor may serve for clustering shapes into semantically coherent parts. In *shape retrieval*, the descriptors are used in several ways to define shape signatures [20]. For example they can allow to represent a shape as a collection of "geometric words" [21]. In this paper, we introduce a novel shape descriptor called the Wave Kernel Signature which is significantly more discriminative than previous approaches.

1.1. Related Work

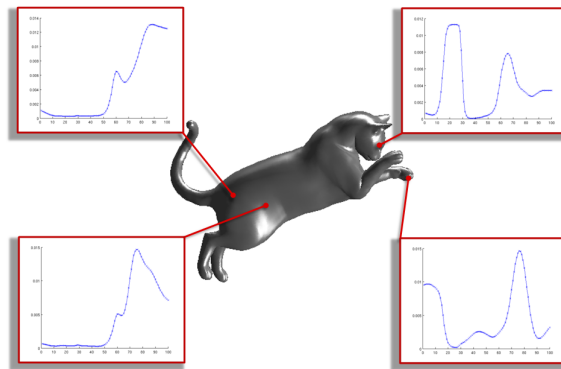Existing descriptors can be roughly divided in two classes according to the level of invariance they have. The

Figure 1. Schrödinger's cat [24] and its Wave Kernel Signatures. Based on the Schrödinger equation each point on an object's surface is associated with a Wave Kernel Signature. Note that the signature captures shape variations in the environment of the considered point at various spatial scales: While the two points of the bottom are quite similar for large scales (small values of the energy), the two others are quite different.

more classical approaches like Shape Context [3] or the Spin Images [12] are invariant under rigid motion. Such descriptors also include the Integral Invariants [19], the Multiscale Local Signature [14] and the Point-Aware Metric [18].

More recently researchers considered descriptors which are invariant under non-rigid motion. Examples include [15, 11, 8], who used ideas similar to the Shape Context in a geodesic distance framework. Lipman et al. [17, 16] suggested to compare neighborhoods of points in the framework of conformal geometry.

Most related to our approach is a variety of works from the non-rigid category which are based upon the spectrum of the Laplace–Beltrami operator on the surface. These techniques were introduced to the geometry processing community by Lévy [13]. Precursors using the (Euclidean) Laplace operator in the interior of the shape were developed by Tari et al. [27, 26] and by Gorelick et al. [10]. Inspired by the work [4], Rustamov [23] used the Laplace eigenfunctions to define an embedding of the surface in the space of convergent sequences $\ell^2(\mathbb{R})$. This embedding has the

nice property of containing all intrinsic information of each point, its drawback is that it depends on the choice of a basis of eigenfunctions. Even in the case of non-repeated eigenvalues of the Laplace–Beltrami operator there is a sign to choose for each component. This problem was resolved by the introduction of the Heat Kernel Signature [25, 9] and its scale-invariant version [7]. The heat kernel is intimately related to the diffusion distance between points which has been used intensively for shape analysis recently (cf. e.g. [6]).

1.2. Heat Equation and Heat Kernel Signature

The Heat Kernel Signature (HKS) is based on analyzing the heat diffusion process on the shape governed by the equation:

$$\frac{\partial u}{\partial t}(x,t) = \Delta u(x,t). \tag{1}$$

Let $E_0 = 0 > -E_1 \geq -E_2, \ldots$ denote the eigenvalues of the Laplace–Beltrami operator Δ, and let $\phi_k(x)$ denote the corresponding normalized eigenvectors.

The idea of the Heat Kernel Signature is to focus on the following phenomenon: Suppose that at time $t = 0$ all the heat energy is concentrated in a point x. Which amount of heat energy remains at the same point x for time $t > 0$? The mathematical solution to this problem is:

$$\text{HKS}(x,t) = k_t(x,x), \tag{2}$$

where k_t is the heat kernel:

$$k_t(x,y) = \sum_{k=1}^{\infty} e^{-E_k t} \phi_k(x)\phi_k(y). \tag{3}$$

From the point of view of signal processing, the HKS has the following interpretation: The Laplace eigenfunctions are the natural generalization of the Fourier basis. If a point $x \in X$ is interpreted as a signal by means of its delta function δ_x, then $\text{HKS}(x,t)$ is an expression in the squared Fourier coefficients $\phi_k^2(x)$ of δ_x. While the Fourier coefficients $\phi_k(x)$ depend on the choice of the sign of the eigenfunctions and of the ordering in case of repeated eigenvalues, $\text{HKS}(x,t)$ does not. This is an important property when comparing two different shapes.

The SHREC benchmark [5] proves that the HKS is currently the state of the art feature descriptor.

1.3. Open Challenges

Despite its success and elegant physical interpretation, the Heat Kernel Signature and its extension suffer from a number of drawbacks:

- The HKS of a point $x \in X$ is a collection of low-pass filters parametrized over the time t. The larger t, the more high frequencies are suppressed. In this

way, HKS mixes information from various different frequencies in an intransparent way.

- The HKS is highly dominated by information from low frequencies, which correspond to macroscopic properties of the shape. This is devastating for applications like high-precision matching where small scale information plays a crucial role.

- The time parameter and its discrete version play a central role in this kernel. Yet although it is related to scale, it does not have any straightforward interpretation with respect to properties of the shape itself. Thus, the appropriate choice of the time segment and of a logarithmic discretization is a purely heuristic choice validated merely by experiments.

1.4. Contribution

In this paper, we introduce a novel shape descriptor which is derived from studying shape in the framework of Quantum Mechanics. Rather than considering the heat equation, we consider the Schrödinger equation governing the temporal evolution of quantum mechanical particles. We introduce an analogous Wave Kernel Signature (WKS) which like the HKS is invariant to isometries and robust to small non-isometric deformations. Yet it resolves the above limitations of the HKS. In particular:

- As a collection of smoothed delta filters parametrized over frequencies rather than time, the WKS clearly separates the influence of the different frequencies and therby of different spatial scales.

- Since the WKS allows access even to very high frequency information, it gives rise to substantially more accurate matching than the HKS.

- The appropriate choice of parameterization of the WKS arises naturally from a theoretical stability analysis. In this way, WKS is optimized for analyzing shapes undergoing non-rigid deformations.

Quantitative results on two different datasets show that the WKS is significantly more accurate than the currently leading HKS. In numerous experiments, we demonstrate the usefulness of the WKS for 3D shape analysis as well as its robustness to perturbed data.

An application of the WKS to pose-consistent shape segmentation was presented in [1].

2. The Wave Kernel Signature

In this section we introduce the Wave Kernel Signature. The basic idea is to characterize a point $x \in X$ by the average probabilities of quantum particles of different energy
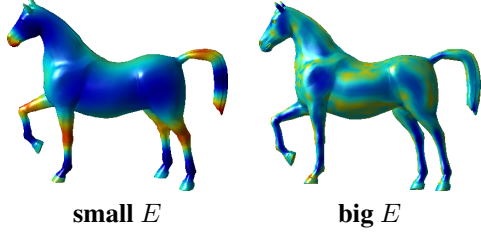
small E **big E**

Figure 2. The key idea is to compute the average probability (over time) to measure a particle with an energy distribution f_E at the location x. The two figures above show the result for two different values of E. Red correspond to high probabilities

levels to be measured in x. Since energies of particles correspond to frequencies, in this approach information from all frequencies is captured while at the same time influences from different frequencies are clearly separated.

We will start in Section 2.1 by determining the probability of measuring a quantum particle of a certain energy distribution in a given location. In Section 2.2, we will perform a theoretical stability analysis which leads us to a choice of the energy uncertainty which is adapted to non-rigid shape analysis. In Section 2.3 we will define the WKS and in Section 2.4 we will outline some of its most important properties.

2.1. Schrödinger's Equation and Energy Measurement

The evolution of a quantum particle on the surface is governed by its wave function $\psi(x, t)$ which is a solution of the Schrödinger equation:

$$\frac{\partial \psi}{\partial t}(x, t) = i \Delta \psi(x, t) \tag{4}$$

Although superficially similar to the heat equation the induced dynamics are drastically different (oscillations rather than mere dissipation).

Consider the following physical experiment: A quantum particle with unknown position is on the surface. At time $t = 0$ we make an approximate measurement of its energy E. We choose here an approximate energy measurement because this will allow us in Section 2.2 to cope with perturbations of eigenenergies under non-rigid deformation of the shape. As a result of this approximate measurement we obtain an energy probability distribution f_E^2 with expectation value E. Assume now that the Laplace spectrum of the shape has no repeated eigenvalues (which is the case with probability 1). Then the wave function of the particle is given by

$$\psi_E(x, t) = \sum_{k=0}^{\infty} e^{iE_k t} \phi_k(x) f_E(E_k). \tag{5}$$

The probability to measure the particle at a point $x \in X$ is then $|\psi_E(x, t)|^2$.

The time parameter has no straightforward interpretation in the characteristics of the shape, so we choose not to consider it. Instead we define the WKS as the average probability (over time) to measure a particle in x:

$$\text{WKS}(E, x) = \lim_{T \to \infty} \frac{1}{T} \int_0^T |\psi_E(x, t)|^2 \tag{6}$$

Since the functions of $e^{-iE_k t}$ are orthogonal for the L^2 norm, we thus have:

$$\text{WKS}(E, x) = \sum_{k=0}^{\infty} \phi_k(x)^2 f_E(E_k)^2 \tag{7}$$

Interestingly in this function, the time parameter has been replaced by energy. This is a very useful aspect because the energy is directly related to the eigenvalues of the Laplace–Beltrami operator and therefore to an intrinsic notion of scale in the shape. To derive a descriptor which characterizes the properties of the shape at different scales independently we merely need to choose the appropriate distributions f_E^2 in (7), and to define an appropriate distance between wave kernels.

2.2. Stability Analysis of Eigenenergies

In the following we will derive an appropriate distribution f_E^2 from a perturbation-theoretical analysis. The key idea is that we want the descriptor to be robust to small non-isometric perturbations of the considered surface while being as informative as possible.

Assume that a surface X is slightly deformed in a non-isometric way. Mathematically we can interpret such a deformation as a perturbation $g(\varepsilon)$ of the metric $g = g(0)$ on X for a real parameter ε with $|\varepsilon|$ small. Assume that the deformation is regular in the sense that $g(\varepsilon) = g(0) + \varepsilon g^1 + \varepsilon^2 g^2 + \ldots$ and the corresponding Laplace–Beltrami operators $\Delta(\varepsilon) = \Delta(0) + \varepsilon \Delta_1 + \varepsilon^2 \Delta_2 + \ldots$ depend analytically on ε (compare also [22, Def. 3]). For simplicity, we assume that the Laplace–Beltrami operator $\Delta(0)$ corresponding to $g(0)$ has no repeated eigenvalues. By [22, Satz 2], for each eigenvalue $-E_k$ of $\Delta(0)$, there exists an analytic family $E_k(\varepsilon)$ with $E_k(0) = E_k$ and $-E_k(\varepsilon)$ in the spectrum of $\Delta(\varepsilon)$.

Proposition. *Denote by $C = ||g^1||_{g(0)}$ the first order norm of the metric deformation, where the space of symmetric tensors $TX^* \otimes TX^*$ is endowed with the norm induced by $g(0)$. Then for $|\varepsilon| > 0$ sufficiently small we have*

$$|E_k(\varepsilon) - E_k| \leq C E_k \cdot |\varepsilon| + \mathcal{O}(\varepsilon^2).$$

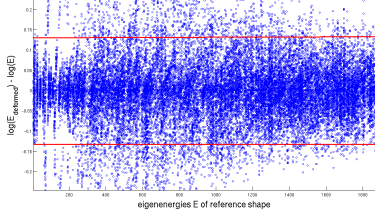*Proof.* The proof is somewhat lengthy and is deferred to our technical report [2]. □

Figure 3. Variation of eigenvalues of the Laplace–Beltrami operator for four articulated shapes (blue circles) in log scale.

The proposition implies that there exist c_k with $|c_k| \leq C$ such that

$$E_k(\varepsilon) = (1 + \varepsilon c_k) E_k + \mathcal{O}(\varepsilon^2).$$

This can be reformulated as

$$\log\left(\frac{E_k(\varepsilon)}{E_k}\right) = \log(1 + \varepsilon c_k + \mathcal{O}(\varepsilon^2)) = \varepsilon c_k + \mathcal{O}(\varepsilon^2). \quad (8)$$

If deformations are independently distributed, we may assume c_k to be normally distributed random variables with zero mean. In view of (8) this implies

$$\log(E_k(\varepsilon)) \sim \mathcal{N}(\log(E_k), \sigma). \quad (9)$$

This assumption is confirmed by the experiments in Figure 3. This reasoning shows that the eigenenergies of an articulated shape X are log-normally distributed random variables. Hence energies in the measurement need to follow the same distribution so that we choose f_E^2 as a log-normal distribution.

2.3. Definition of the Wave Kernel Signature

With the above insights we are now ready to concretize (7). We define the Wave Kernel Signature at a point $x \in X$ as a real valued function in the logarithmic energy scale $e = \log(E)$, writing $C_e = \left(\sum_k e^{\frac{-(e - \log E_k)^2}{2\sigma^2}}\right)^{-1}$

$$\begin{cases} \mathrm{WKS}(x, \cdot) \; : \; \mathbb{R} \to \mathbb{R}, \\ \mathrm{WKS}(x, e) = C_e \sum_k \phi_k^2(x) e^{\frac{-(e - \log E_k)^2}{2\sigma^2}}. \end{cases} \quad (10)$$

To compare Wave Kernel Signatures for different locations $x \in X$ and $y \in Y$ on respective shapes X and Y, we simply define a distance using the L^1 norm of the normalized signature difference:

$$d_{\mathrm{WKS}}(x, y) = \int_{e_{\min}}^{e_{\max}} \left| \frac{\mathrm{WKS}(x, e) - \mathrm{WKS}(y, e)}{\mathrm{WKS}(x, e) + \mathrm{WKS}(y, e)} \right| de \quad (11)$$
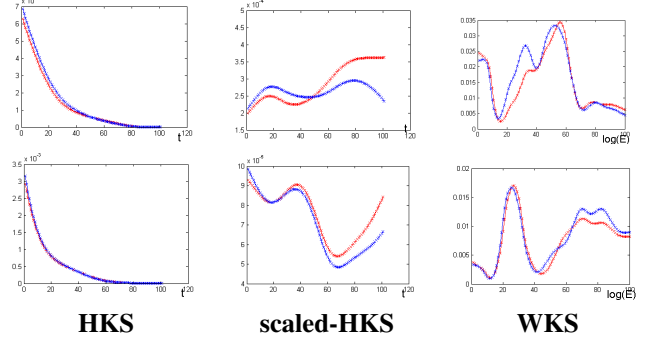

HKS **scaled-HKS** **WKS**

Figure 4. Comparison of the Heat Kernel Signature (first column), the scaled Heat Kernel Signature (second column) and the Wave Kernel Signature (third column) for two different points (first and second line). Note that while remaining robust to deformations the WKS captures more information including shape differences at finer scales.

where $e_{\min} \in \mathbb{R}$ and $e_{\max} \in \mathbb{R}$ correspond to the largest and smallest considered energy scales. The bigger $e_{\max}$, the more local information included.

In all our experiments, the parameters were fixed. We computed $N = 300$ eigenvalues of the Laplacian and we evaluated at $M = 100$ values of e. We used $e_{\min} = \log(E_1) + 2\sigma$, the logarithm of the smallest eigenvalue different from 0 and $e_{\max} = \log(E_N) - 2\sigma$. The increment δ in e was $(e_{\max} - e_{\min})/M$, the variance σ was set to 7δ.

2.4. Properties of the Wave Kernel Signature

The Wave Kernel Signature has a number of properties that make it well suited for shape analysis and shape comparison:

- The WKS is *intrinsic* in the sense that it is invariant to non-rigid motions, i.e. if $T : X \to Y$ is an isometry, then $\mathrm{WKS}(x, e) = \mathrm{WKS}(T(x), e)$ for all $x \in X$.

- The WKS is *informative*: Assume that the Laplace–Beltrami spectrum of two closed surfaces X, Y has no repeated eigenvalues (this is true for every generic shape) and that $T : X \to Y$ is a homeomorphism. Then $\mathrm{WKS}(x, e) = \mathrm{WKS}(T(x), e)$ for all $x \in X$ and $e \in \mathbb{R}$ if and only if T is an isometry. The proof of this statement is analogous to the one in [25].

- The Wave Kernel Signature has a *natural notion of scale* since it is a function of energy levels which are directly related to scales. Large energies correspond to highly oscillatory particles which are mostly influenced by the local geometry whereas small energies correspond to properties induced by the global geometry.

  Mathematically, we can interpret the WKS as a collection of smoothed delta filters on the squared Fourier

HKS

WKS

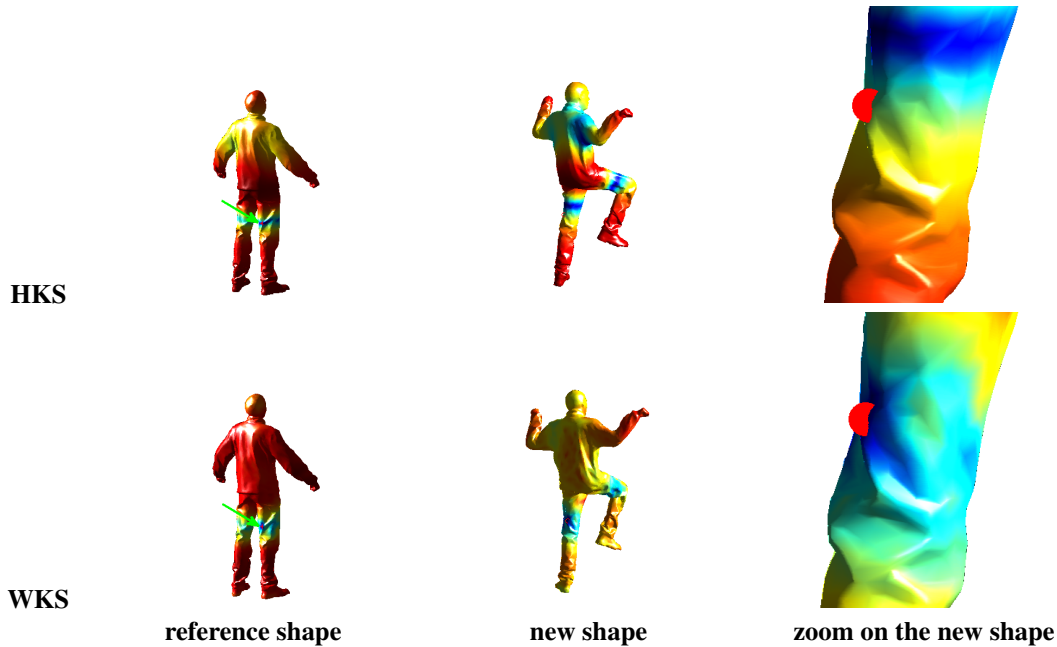| reference shape | new shape | zoom on the new shape |

Figure 5. The figures show the logarithmic distance between the descriptor of a point in the reference frame (on the leg) and the descriptor of other points in the same frame (first column) and in another (second and third column). Since it does not overweight the small eigenvalues the Wave Kernel Signature provides not only a unique correspondence (no false matches at the shoulders obtained with the HKS), but it also provides a more accurate correspondence highly localized around the correct correspondent (shown in the closeup on the right).

coefficients of (delta functions of) points.

- By construction, the WKS is *stable under perturbations of the shape* – see the examples in Figure 4. Thereby, it is well-suited for the analysis of articulated shapes.

- While the physical model and the mathematical stability analysis were presented under the simplifying assumption that the Laplace–Beltrami operator of the shape has no repeated eigenvalues, we note that the WKS is well-defined even in the case of repeated eigenvalues.

- The WKS can easily be made *scale-invariant* as done in [7] for the heat kernel signature. We omit the details because the steps are exactly the same as for the heat kernel, except that the WKS naturally lives in a log space.

3. Experimental Results

In the following we will present both qualitative and quantitative evidence showing that the proposed Wave Kernel Signature is superior to the traditional Heat Kernel Signature. Furthermore, we will show a straight-forward application of the WKS to shape matching.

3.1. Informative Shape Signatures

Figure 4 shows respective signatures of a specific point on the shape before (blue) and after (red) deformation of the shape. In contrast to the HKS and the scaled HKS, the WKS maintains information on several spatial scales indicating on which scales shape changes have occurred: The shape has changed, so signatures should not be identical, yet it is the same point on the shape, so signatures should be sufficiently similar to allow for reliable matching.

Figure 5 shows the distance from the point marked as a red cross to the other points of the same shape and to points from a different shape: it proves that matching is possible even for not specific points (while standard point descriptors only work well for feature points).

3.2. Robustness

For real world applications it is of great importance to dispose of a feature descriptor which is robust to various types of perturbed data. The SHREC feature descriptor benchmark [5] provides a very good dataset for testing such robustness. It includes shapes undergoing a variety of perturbations such as noise, shotnoise, holes, topological changes, scale, and localscale. We tested the Wave Kernel Signature on this data. In general, the WKS proves very stable under perturbations. Even in the strongest transformation classes proposed in the benchmark, we get good correspon-
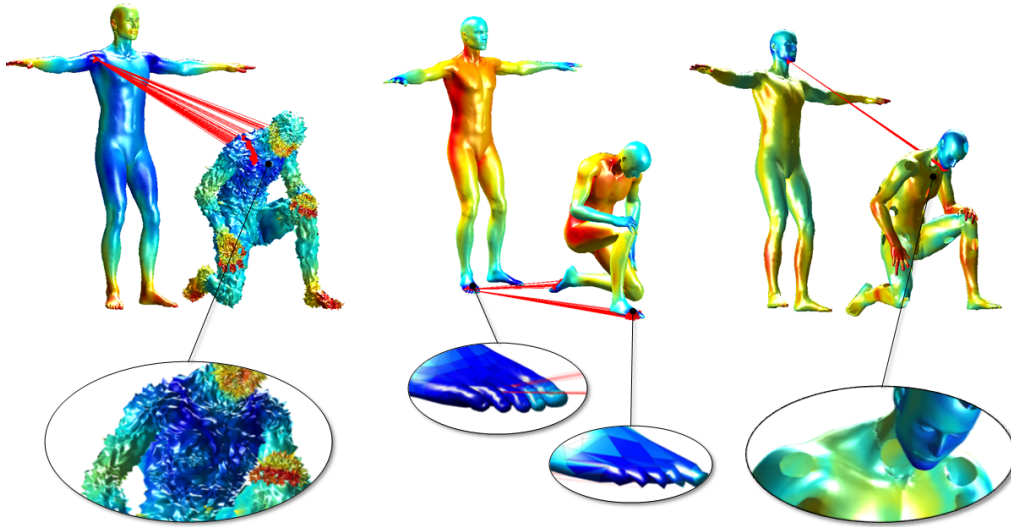
Figure 6. Robustness of the WKS: The red lines connect a reference point on the shape in the background (standing David) with its 50 best matches on the perturbed shape in the foreground (sitting David). The color encodes the feature distance to the reference point, blue indicating proximity and red large distance in the feature space. The experiments visualized here are done with shapes in the strongest perturbation category of the SHREC 2010 feature descriptor dataset. **Left image:** Visibly, the deformed shape is very noisy. WKS can still locate the correspondence of the shoulders. Note that an isometry invariant feature descriptor cannot distinguish the left and the right shoulder. **Middle image:** The reference mesh has 52565 vertices, while the perturbed mesh has 2634 vertices. **Right image:** The deformed shape has many holes.

dences as visualized in Figure 6. There, we show results on the transformation types noise, sampling and holes. The red lines indicate the best 50 correspondences of a reference point on the shape in the background with a perturbed shape.

3.3. Quantitative Comparison

To make the qualitative statements about precision and robustness of our feature descriptor measurable, we compared WKS and HKS regarding their quantitative performance on shape matching. To this end, we evaluated on two different datasets.

- We used the dataset provided by Vlasic et al. [28]. It contains human shapes in a large variety of different poses. To measure the quality of a descriptor we proceeded as follows:

  1. Detect feature points by means of farthest point sampling, i.e. sequentially detect the most distinguished feature points (those which are most distant in feature space). Both for HKS and WKS these feature points typically coincide with characteristic surface locations that humans would select (i.e. the head, the hand, the foot, etc.) – see Figure 7.

2. For each of these reference points, select the k best matches on a deformed shape, k running from 1 to $N/100$. Here, N is the number of vertices on the deformed mesh.

3. Plot the hit rate, that is the percentage of feature points for which the correct correspondent is among the k best matches. On the x-axis we choose the percentual scale $100 \cdot k/N$ which allows for comparisons between meshes in different resolutions.

The left graph in Figure 8 shows the hit rate for increasing values of $100 \cdot k/N$ obtained for the (scaled) HKS as proposed by Sun et al. [25] in their implementation and the WKS. This evaluation shows that the matching precision of the WKS is clearly superior to that of the HKS, finding for about 87 % of the reference points their correspondents among the first 1 % of the best matches.

- Evaluation on the SHREC 2010 benchmark dataset [5]. The evaluation on this data allows us to quantify the robustness of our descriptor to perturbed data. Again, we used the hit rate as a quality measure.

The right graph in Figure 8 shows the result on this benchmark. While of course on data underlying such
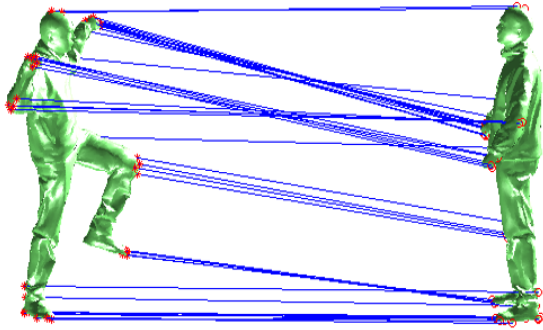
Figure 7. Matching result using the Wave Kernel Signature with the algorithm outlined in 3.4 with 40 feature points selected on the left shape. Using these points, it is the easy to compute a dense matching using geodesic distances for all other points. Yet, such a dense matching is difficult to visualize.

challenging transformations, the results are less accurate than on the Vlasic dataset, we see that the hit rate of the WKS is still substantially above the hit rate of the HKS, achieving 63 % of correct correspondences among the first 1 % of best matches.

3.4. Shape Matching

Estimating a dense spatially regularized matching of two $3D$ shapes is a difficult computational challenge which is beyond the scope of this work. Nevertheless we will demonstrate that the proposed WKS is sufficiently informative so as to compute a meaningful matching of $3D$ shapes using the following simple and greedy strategy:

1. For both shapes select the N most discriminative feature points.

2. For each feature point on one shape select the k best matching feature points on the other shape.

3. Select as first corresponding pair the one with smallest feature distance.

4. Iteratively match pairs of points for which the geodesic distances to the already matched points are most similar. This last aspect introduces the regularity into the matching.

Figure 7 shows a matching computed with the above algorithm for a human figure in two different poses. It is straight-forward to extend this matching to all points of the

mesh starting from this sparse matching, yet we omit such dense matching results here as they are not easily visualized.

4. Conclusion

Based on a quantum mechanical approach to shape analysis, we introduced the Wave Kernel Signature (WKS) as a novel feature descriptor. As the Heat Kernel Signature (HKS), it is based on the Laplace–Beltrami operator and carries a physical interpretation: While the HKS arises from studying the heat equation on the surface, the WKS arises from studying the Schödinger equation governing the dissipation of quantum mechanical particles on the geometric surface. In contrast to the HKS, the WKS clearly separates influences of different frequencies, treating all frequencies equally. Appropriate parameterization of the WKS is determined by a theoretical stability analysis aiming at features which are both highly informative yet robust to non-isometric perturbations of the shape. Experimental results confirm that due to a better separation of scales and a better access to fine scale information, the WKS allows for substantially more accurate feature matching than the HKS. Even with strongly perturbed data, the WKS can still correctly detect feature correspondences. We demonstrated the usefulness of the WKS for computing shape matching.

5. Acknowledgement

References

[1] M. Aubry, U. Schlickewei, and D. Cremers. Pose-consistent 3d shape segmentation based on a quantum mechanical feature descriptor. In R. Mester and M. Felsberg, editors, *Proc. 33rd DAGM Symposium*, LNCS, Frankfurt, Germany, 2011. Springer. 2

[2] M. Aubry, U. Schlickewei, and D. Cremers. The wave kernel signature:a quantum mechanical approach to shape analysis. In *Technical report, TU München*, Germany, 2011. 3

[3] S. Belongie, J. Malik, and J. Puzicha. Shape context: A new descriptor for shape matching and object recognition. In *Proc. Neural Information Processing Systems*, 2000. 1

[4] P. Bérard, G. Besson, and S. Gallot. Embedding Riemannian manifolds by their heat kernel. *Geometric and Functional Analysis*, 4(4):373–398, 1994. 1

[5] A. Bronstein, M. Bronstein, B. Bustos, U. Castellani, M. Crisani, B. Falcidieno, L. Guibas, I. Kokkinos, V. Murino, M. Ovsjanikov, et al. SHREC 2010: robust feature detection and description benchmark. *Proc. 3DOR*, 2010. 2, 5, 6, 8

[6] A. Bronstein, M. Bronstein, R. Kimmel, M. Mahmoudi, and G. Sapiro. A Gromov-Hausdorff framework with diffusion geometry for topologically-robust non-rigid shape matching.
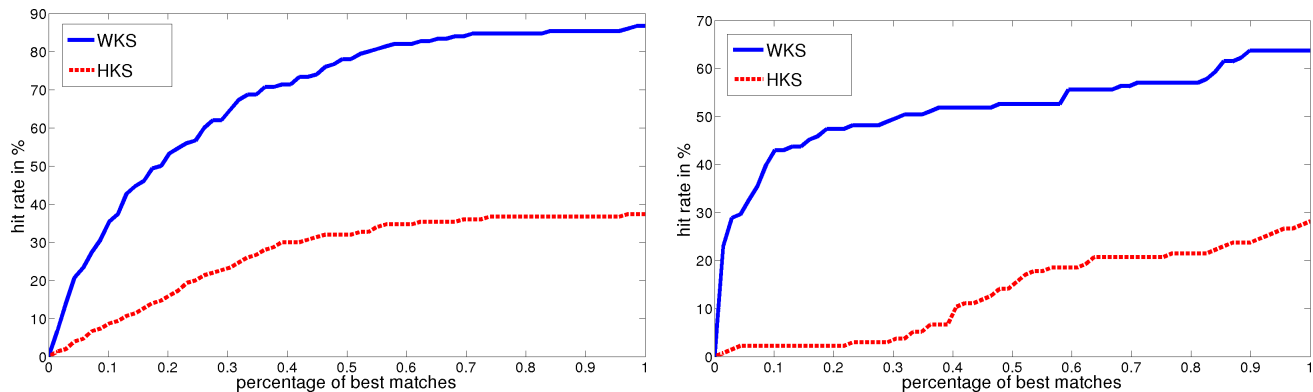
Figure 8. Quantitative comparison of the matching performance of HKS and WKS. **Left graph:** We considered two very different shapes of the "Crane" dataset in [28] and chose feature points on one of them. For various values of $100 \cdot k/N$, N being the number of vertices, we plotted the hit rate for finding the true correspondent among the first k matches. The hit rate of the WKS is clearly superior to that of the HKS. **Right graph:** Hit rate on the 2010 SHREC benchmark with shapes perturbed by 9 challenging transformations such as noise, topology changes, holes and changes in the local or global scale. [5] The qualitative behaviour of WKS against HKS is the same as on the Vlasic dataset. However, due to the strong perturbations of the input data, the results are less accurate. For 63 % of the reference points, WKS is able to detect the correct corresponding points among the first 1 % of the best matches on the perturbed meshes.

International Journal of Computer Vision, 89(2):266–286, 2010. 2

[7] M. Bronstein and I. Kokkinos. Scale-invariant heat kernel signatures for non-rigid shape recognition. In *Proc. International Conference on Computer Vision and Pattern Recognition*, pages 1704–1711. IEEE, 2010. 2, 5

[8] R. Gal and D. Cohen-Or. Salient geometric features for partial shape matching and similarity. *Transactions on Graphics (TOG)*, 25(1):130–150, 2006. 1

[9] K. Gebal, J. Bærentzen, H. Aanæs, and R. Larsen. Shape analysis using the auto diffusion function. *Computer Graphics Forum*, 28(5):1405–1413, 2009. 2

[10] L. Gorelick, M. Galun, E. Sharon, R. Basri, and A. Brandt. Shape representation and classification using the poisson equation. *IEEE PAMI*, pages 1991–2005, 2006. 1

[11] M. Hilaga, Y. Shinagawa, T. Kohmura, and T. Kunii. Topology matching for fully automatic similarity estimation of 3D shapes. In *Proc. annual conference on Computer graphics and interactive techniques*, pages 203–212. ACM, 2001. 1

[12] A. Johnson and M. Hebert. Using spin images for efficient object recognition in cluttered 3D scenes. *IEEE PAMI*, 21(5):433–449, 2002. 1

[13] B. Lévy. Laplace-Beltrami Eigenfunctions Towards an Algorithm That. In *Proc. Int. Conf. on Shape Modeling and Applications*, page 13. IEEE, 2006. 1

[14] X. Li and I. Guskov. Multi-scale features for approximate alignment of point-based surfaces. In *SGP*, page 217. Eurographics, 2005. 1

[15] H. Ling and D. Jacobs. Shape classification using the inner-distance. *IEEE PAMI*, pages 286–299, 2007. 1

[16] Y. Lipman and I. Daubechies. Surface Comparison with Mass Transportation. *Arxiv preprint arXiv:0912.3488*, 2009. 1

[17] Y. Lipman and T. Funkhouser. Möbius voting for surface correspondence. *Transactions on Graphics (TOG)*, 28(3):1–12, 2009. 1

[18] R. Liu, H. Zhang, A. Shamir, and D. Cohen-Or. A Part-aware Surface Metric for Shape Analysis. *Computer Graphics Forum*, 28(2):397–406, 2009. 1

[19] S. Manay, D. Cremers, B.-W. Hong, A. Yezzi, and S. Soatto. Integral invariants for shape matching. *IEEE PAMI*, 28(10):1602–1618, 2006. 1

[20] R. Osada, T. Funkhouser, B. Chazelle, and D. Dobkin. Shape distributions. *Transactions on Graphics (TOG)*, 21(4):807–832, 2002. 1

[21] M. Ovsjanikov, A. Bronstein, M. Bronstein, and L. Guibas. Shape Google: a computer vision approach to invariant shape retrieval. *Proc. NORDIA*, 1(2), 2009. 1

[22] F. Rellich. Störungstheorie der Spektralzerlegung. *Mathematische Annalen*, 113:600–619, 1937. 3

[23] R. Rustamov. Laplace-Beltrami eigenfunctions for deformation invariant shape representation. In *SGP*, pages 225–233. Eurographics, 2007. 1

[24] E. Schrödinger. Die gegenwärtige Situation in der Quantenmechanik. In *Naturwissenschaften*, 1935. 1

[25] J. Sun, M. Ovsjanikov, and L. Guibas. A Concise and Provably Informative Multi-Scale Signature Based on Heat Diffusion. *Computer Graphics Forum*, 28(5):1383–1392, 2009. 2, 4, 6

[26] S. Tari and J. Shah. Nested Local Symmetry Set* 1. *Computer Vision and Image Understanding*, 79(2):267–280, 2000. 1

[27] Z. Tari, J. Shah, and H. Pien. Extraction of shape skeletons from grayscale images. *Computer Vision and Image Understanding*, 66(2):133–146, 1997. 1

[28] D. Vlasic, I. Baran, W. Matusik, and J. Popović. Articulated mesh animation from multi-view silhouettes. In *ACM SIGGRAPH 2008 papers*, pages 1–9. ACM, 2008. 6, 8